Article

J. Biol. Regul. Homeost. Agents. 2024; 38(5): 4119–4130
https://doi.org/10.23812/j.biol.regul.homeost.agents.20243805.327

Deubiquitinase Inhibitor AuPT Downregulates NF-κB Signaling and Induces Apoptosis via Inhibiting UCHL5 and USP14 in Prostate Cancer

Hongwei Zhang[1,†], Ping Zhou[2,†], Xiaohong Feng[3], Dandan Chen[4], Ping Tang[3,*]

[1]Organ Transplantation Department, Changde Hospital, Xiangya School of Medicine, Central South University, The First People's Hospital of Changde City, 415003 Changde, Hunan, China
[2]School of Basic Medical Sciences, Guangzhou Medical University, 511436 Guangzhou, Guangdong, China
[3]Urology Department, Guangzhou First People's Hospital, 510180 Guangzhou, Guangdong, China
[4]Emergency Department, Guangzhou First People's Hospital, 510180 Guangzhou, Guangdong, China
*Correspondence: sytangping@aliyun.com (Ping Tang)
[†]These authors contributed equally.
Published: 1 May 2024

Background: Deubiquitinases (DUBs) are essential components of the ubiquitin-proteasome system (UPS) that regulates cancer-related processes. Effective inhibitors of 19S proteasome-associated DUBs, including ubiquitin carboxy-terminal hydrolase L5 (UCHL5), ubiquitin-specific protease 14 (USP14), and gold-(triphenylphosphine (PPh3))-platinum (AuPT), suppress cell growth in several human tumor cell lines. The aim of this study was to determine the effect of AuPT and its mechanism of action on prostate cancer (PCa) progression.

Methods: The malignant PCa phenotype and apoptotic cell death were evaluated *in vitro*. The antitumor activity of AuPT was verified using nude xenografts. Furthermore, the protein levels in the UPS and the phosphorylation of p65 were determined by overexpression plasmid transfection using Western blotting.

Results: The viability, invasion, and migration abilities of PCa cells decreased and the cell apoptosis rate increased with AuPT treatment in a time-dependent manner ($p < 0.05$, $p < 0.01$). The tumor weight and volume were effectively suppressed in nude mice ($p < 0.01$). DUB protein expression levels and p65 phosphorylation were downregulated and restored after overexpression of USP14 or UCHL5 ($p < 0.05$, $p < 0.01$, $p < 0.001$).

Conclusions: We found that AuPT induced PCa cell apoptosis and inhibited the activation of nuclear factor-κB (NF-κB) signaling by disturbing UPS functioning. AuPT treatment may enable specific targeted therapy against NF-κB-activated PCa.

Keywords: prostate cancer; AuPT; NF-κB signaling; UCHL5 and USP14; apoptosis

Introduction

Prostate cancer (PCa) is the second most common type of cancer in men after lung cancer [1]. A recent epidemiological study estimated that approximately 1.4 million cases and 375,000 deaths were associated with PCa worldwide in 2020 [2]. PCa incidence is differs geographically, being prevalent in northern and western Europe and America [3]. Preventive measures, including screening for prostate-specific antigens, can substantially reduce the incidence and mortality of PCa [4]. PCa can develop into castration-resistant PCa after some patients receive androgen deprivation therapy, which involves treatment with androgen receptor (AR) inhibitors such as enzalutamide or abiraterone to attenuate PCa progression [5,6]. However, resistance to chemotherapy rapidly occurs in patients with PCa [7]. Therefore, new and effective drugs for the treatment of PCa must be identified.

Deubiquitinases (DUBs) are crucial regulatory factors of the ubiquitin-proteasome system (UPS) in eukaryotes. DUBs protect cellular proteins from ubiquitination-mediated degradation by hydrolyzing ubiquitin chains [8]. The human gene encodes approximately 100 DUBs, which are classified into six families based on different cysteine residues [9]. Among these, regulatory particle subunit 11, ubiquitin-specific protease 14 (USP14), and ubiquitin carboxy-terminal hydrolase L5 (UCHL5) are related to 19S regulatory particles and regulate proteasome degradation [10]. Abnormal DUB expression is closely related to the progression of human cancers [11–13]. Considering the involvement of UPS regulators in various cancer pathways, using UPS as a drug target may advance anticancer therapies.

The nuclear factor-κB (NF-κB) pathway is a highly conserved stress-responsive pathway that regulates multiple biological processes, including carcinogenic signals

Journal of
BIOLOGICAL REGULATORS
and Homeostatic Agents

[14]. The canonical NF-κB signaling pathway promotes cancer progression through a high-level inflammation response in the cancer microenvironment and the elevated expression of proangiogenic genes and chemokines [15]. Additionally, the UPS can control the activation of the NF-κB transcription factor pathway, where the level of ubiquitination among its components is high [16]. DUB can regulate the growth of various tumors through the NF-κB signaling pathway [17–19]. Thus, DUB inhibitors targeting the NF-κB pathway may be effective as cancer therapy.

The identification of the biological activity of cisplatin was a critical milestone in the development of metal-based anticancer medicine [20]. To date, some metal-based compounds strongly inhibit DUBs and induce apoptosis in cancer cell lines [21]. However, treatments with platinum-based agents are frequently associated with serious side effects [22]. Therefore, effective metal-based DUBs inhibitors need to developed as anticancer drugs. Previously, we synthesized a new gold (I) complex, gold-(triphenylphosphine (PPh3))-platinum (AuPT), and a metal-based drug as a DUB inhibitor that selectively suppresses the growth of cells from patients with acute myeloid leukemia and lung cancer xenografts in nude mice, and the cytotoxicity of the drug was low [23]. However, whether AuPT has similar effects on PCa remains unclear.

Studies on the role of AuPT and the potential mechanisms involved in PCa are lacking. In our study, by combining *in vivo* and *in vitro* experiments, we evaluated the antitumor potential mechanism that is involved in the therapeutic effects of AuPT on PCa.

Materials and Methods

Cell Culture

Human PCa cell line PC3 cells (22Rv1, iCell, Shanghai, China) were seeded in Ham's medium F-12K (F12K, 0007, iCell, Shanghai, China) supplemented with 10% fetal bovine serum (FBS, 2020010501, iCell, Shanghai, China) and antibiotics (100 IU/mL penicillin G and 100 µg/mL streptomycin, SV30082.01, HyClone, Logan, UT, USA). Then, the cells were cultured in an incubator at 37 °C in a 5% CO_2 atmosphere. All cells were mycoplasma-free and authenticated using short tandem repeat DNA profiling. The STR identification profile of the cell line is provided in the **Supplementary Supporting Information**.

Cell Viability Assay

A cell counting kit-8 (CCK-8) assay (CA1210; Solarbio, Beijing, China) was used to measure the viability of PC3 cells. PC3 cells were seeded in 96-well microplates (1×10^4 cells/well). Next, F12K medium supplemented with 10% FBS was added to the culture cells for 24 h. Then, cells were treated with a certain concentration of AuPT (1, 2, 4, 6, or 8 µM) and co-cultivated for 24 h or treated with 2 µM AuPT and co-cultivated for 3, 6, 9, 12, and 24 h. Then, 90 µL of cells was stained with 10 µL of CCK-8 reagent from each well, which was followed by co-culturing for 2 h. The absorbance was measured at 450 nm using a microplate reader (VL0000D0, Thermo Fisher Scientific, Waltham, MA, USA). Cell viability was calculated as: Cell viability (%) = [A (with different AuPT dosing) – A (blank)]/[A(without AuPT dosing) – A (blank)] × 100%. This experiment was repeated three times.

Cell Wound Healing Assay

A total of 5×10^5 PC3 cells/well were seeded into a 6-well plate and cultured in complete medium. When the confluency of cells reached 80%, the cell monolayers were scratched with a 100 µL sterile pipette tip. The scratched cells were washed with phosphate-buffered saline (PBS) three times. The remaining cells were incubated with serum-free F12K medium, and the scratch was immediately recorded at 0 h. At 0, 12, 15, 18, and 21 h after scratching, 2 µM AuPT was added to cells for 3, 6, 9, 12, or 24 h of treatment in an incubator at 37 °C in a 5% CO_2 atmosphere. Wound width was measured to reflect the process of cell wound healing *in vitro*, and the wound was photographed using an inverted microscope (Eclipse 80i, Nikon, Tokyo, Japan) at the indicated times. The wound healing rate was calculated as [(scratch width at 0–24 h)/0 h scratch width] × 100%.

Cell Invasion Assay

The invasive ability of PC cells is often assessed using a Transwell invasion assay *in vitro*. Briefly, 100 µL of 1:8 F12K medium-diluted Matrigel (C08383, Beyotime, Shanghai, China) was added to each well at 37 °C for 30 min. Next, approximately 5×10^5 PC3 cells/well were seeded in the upper chamber of 24-well plates containing 100 µL of free-serum F12K medium; then, 600 µL of F12K medium supplemented with 20% FBS was added into the lower chamber. After 24 h of incubation at 37 °C, the upper chamber was removed, and invasive cells on the surface of the lower chamber were washed with PBS, fixed with 4% paraformaldehyde solution for 30 min, and stained with 0.1% crystal violet solution for 20 min. The cells that passed through the filter were counted in five random fields under a microscope (Eclipse 80i, Nikon, Tokyo, Japan). Each experiment was repeated three times.

Cell Apoptosis

PC3 cells were seeded into 6-well plates (5×10^5 cells/well in l mL) in F12K medium containing 10% FBS for 24 h. After treatment with 2 µM AuPT for different durations (3, 6, 9, 12, and 24 h), cells were collected using trypsin without EDTA, washed with PBS, and resuspended in binding buffer. Next, 100 µL of cells was inoculated with 5 µL of Annexin V-Fluorescein Isothiocyanate (V-FITC) at room temperature for 5 min in the dark. Then, cells were stained with propidium iodide (ST512, Beyotime, Shang-

hai, China) and resuspended with 400 µL of PBS. The rate of apoptosis was determined using flow cytometry (342973, BD Biosciences, San Jose, CA, USA). This experiment was repeated three times.

Western Blotting Assay

The protein expression levels of BCL2-associated X (Bax), B-cell lymphoma-2 (Bcl-2), caspase-3, UCHL5, USP14, p27, p53, C/EBP-homologous protein (CHOP), Heavy-chain binding protein (Bip), and NF-κB p65 were measured via Western blotting. The total protein was extracted from the treated cells using RIPA buffer, and the protein lysates were separated using SDS-PAGE and transferred onto a PVDF membrane (IPVH00010, Millipore, Danvers, MA, USA). After blocking with 5% nonfat milk at room temperature for 2 h, the membrane was incubated with primary antibodies (Abcam, Cambridge, UK) as follows: anti-Bax, ab32503, 1:2000; anti-Bcl-2, ab32124, 1:2000; anti-caspase-3, ab32351, 1:1000; anti-UCHL5, ab192616, 1:2000; anti-USP14, ab137433, 1:2000; anti-p27, ab32034, 1:2000; anti-p53, ab32049, 1:2000; anti-CHOP, ab11419, 1:2000; anti-Bip, ab21685, 1:2000; anti-NF-κB p65, ab32536, 1:2000; and anti-β-actin, ab8226, 1:2000 at 4 °C for 12 h. After washing four times with Tris-buffered saline containing Tween, the membrane was incubated with horseradish-peroxidase-conjugated secondary antibodies including anti-rabbit (IgG, A0216, Beyotime, Shanghai, China) or anti-mouse (1:5000, A0208, Beyotime, Shanghai, China) at room temperature for 1 h. Finally, the immunoblot was colored using enhanced chemiluminescence and visualized using an imaging system (Tanon 5200, Tanon Science and Technology, Shanghai, China). The band images were quantified using Image J software (V1.8.0.112, NIH, Madison, WI, USA) with β-actin used as the internal control.

Construction of a Mouse Model of PCa

All animal experiments were approved by the Institutional Animal Care and Use Committee of the Guangzhou Medical University (approval number: GY2018-043). Healthy adult nude mice (BALB/c, male, 6–8 weeks old, 20–22 g, $n = 18$) were purchased from Guangdong Animal Center and housed in standard cages at a specific pathogen-free level on a 12 h light/dark cycle at a constant temperature of 22–26 °C with a relative humidity of 50–55%. After one week of acclimatization with free access to rodent food and autoclaved water, 18 nude mice were subcutaneously injected with PC3 cells to induce cancer and then randomly divided into three different groups ($n = 6$/group): control group, low-dose AuPT (3 mg/kg) group, and high-dose AuPT (6 mg/kg) group. The control and experimental groups received normal saline and AuPT, respectively, daily for four weeks via oral gavage. Tumor length (a) and width (b) were measured using a Vernier caliper once per week to record tumor volume using the following formula: $1/2 \times (a \times b^2)$. Finally, the mice were euthanized using an intraperitoneal injection of sodium pentobarbital (50 mg/kg, P3761, Sigma-Aldrich, St. Louis, MO, USA), and tumor tissues were collected to measure tumor volume and weight for further experiments.

Immunohistochemistry

The tumor tissues collected from each treatment group were fixed with 4% paraformaldehyde solution for 24 h and embedded in paraffin. The maximum cross-section of the paraffin-embedded tumor tissue for staining was 4 µm. After the sections were deparaffinized and rehydrated with different concentrations of ethanol, they were heated with 10 mM sodium citrate buffer in a microwave for 5 min to recover the antigenic activity. Sections were then incubated with 0.3% hydrogen peroxide at 4 °C for 30 min and blocked with 3% bovine serum albumin at room temperature for 30 min. The serial sections were then incubated with primary antibody anti-ki67 (1:200, ab16667, Abcam, Cambridge, UK) at 4 °C overnight and secondary antibodies (anti-rabbit IgG, 1:200, A0208, Beyotime, Shanghai, China) at room temperature for 80 min. Finally, the sections were stained with diaminobenzidine, counterstained with hematoxylin, and sealed in liquid paraffin. The stained sections were observed by randomly selecting five high-power fields for each mouse (original magnification 200×) using a microscope (Eclipse 80i, Nikon, Tokyo, Japan).

Transfection

UCHL5 or USP14 were overexpressed using plasmid transfection. First, a UCHL5 or USP14 coding sequence was cloned into pcDNA3.1 to overexpress UCHL5 or USP14. An overexpression-Negative Control (oe-NC) was used. PC3 cells were seeded into 24-well plating medium for 24 h with 30%–50% density. 2 h before transfection, PC3 cells were cultured in antibiotic-free complete medium. Then, oe-UCHL5/oe-USP14/oe-NC and Lipo3000 transfection reagent (L3000001, Thermo Fisher Scientific, Waltham, MA, USA) were mixed in antibiotic-free complete medium in a 1:1 radio in aseptic centrifuge tubes, and 50 µL of the mixture was added into each well. After transfection for 6 h, the cells were cultured in fresh complete medium to increase transfection efficiency.

Statistical Analysis

Statistical analyses were performed using GraphPad Prism software (version 7.0; GraphPad, San Diego, CA, USA). Data are presented as mean ± standard deviation. Multiple group comparisons were performed using one-way analysis of variance (ANOVA), which were subsequently analyzed using Tukey's multiple comparison test. Comparisons between two groups were performed using *t*-tests. Each experiment was repeated three times. $p < 0.05$ was considered statistically significant.

Journal of
BIOLOGICAL REGULATORS
and Homeostatic Agents

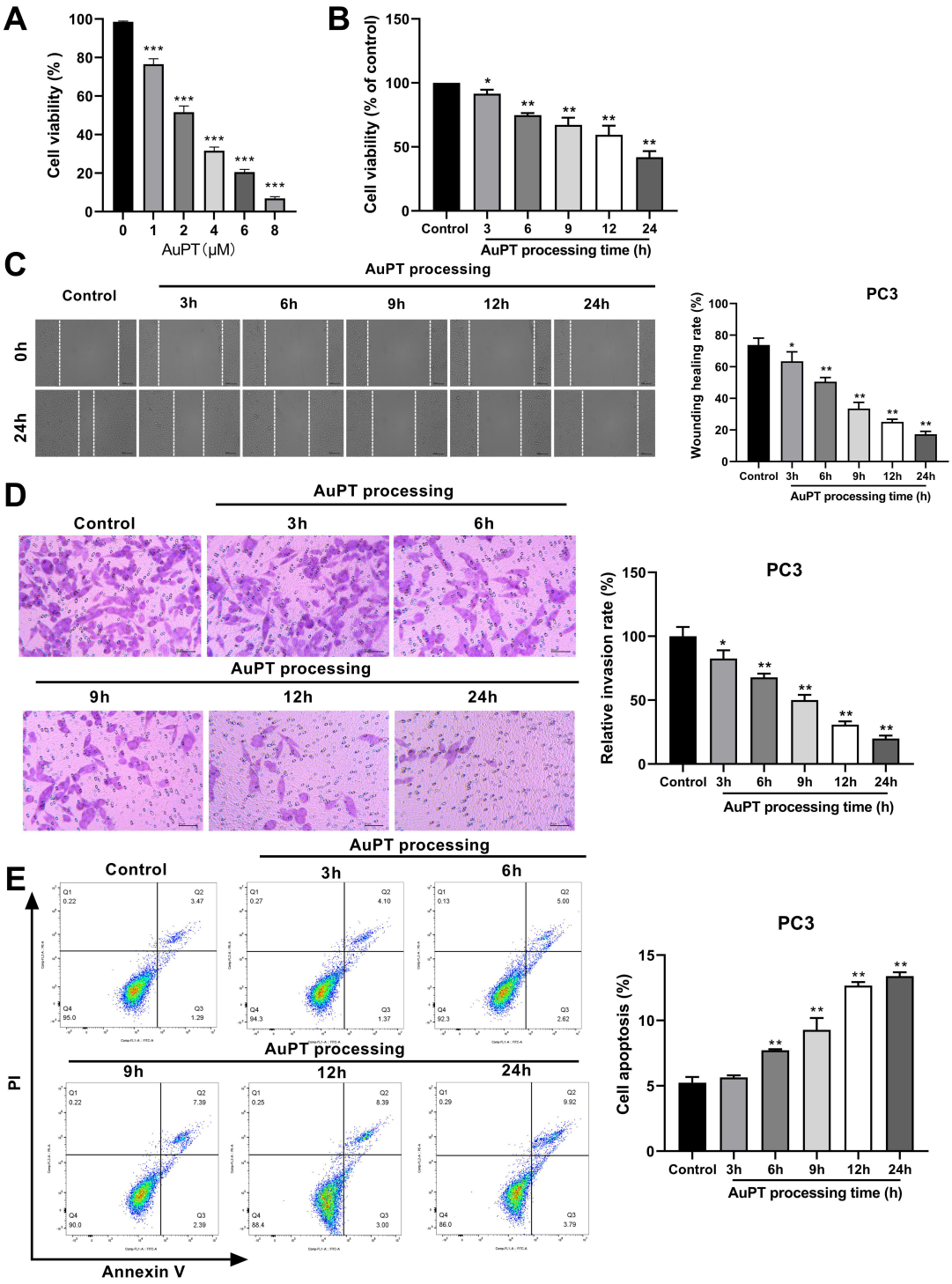

Fig. 1. A gold-(triphenylphosphine (PPh3))-platinum (AuPT) reduces malignant phenotype of human prostate cancer (PCa) cell and promotes cell apoptosis in a time-dependent manner. Relative viability of human PCa cell line PC3 cells treated with different concentrations of AuPT for 24 h (A) or treated with 2 μM AuPT at the time of 3 h, 6 h, 9 h, 12 h and 24 h (B). (C) Cell wound healing assay analysis of the migration capacity of human PC3 cells after AuPT treatment (scale bar: 100 μm). The horizontal represented the process of AuPT treatment (from left to right): the non-AuPT treatment and after 3 h, 6 h, 9 h, 12 h and 24 h of AuPT treatment. The vertical indicated representative photographs at the cells scratch of 0 h and 24 h. (D) Transwell assay analysis of the invasion capacity of human PC3 cells (scale bar: 200 μm). (E) Flow cytometry analysis of the apoptosis of human PC3 cells by staining with Annexin V-FITC and PI after 3 h, 6 h, 9 h, 12 h and 24 h of AuPT treatments. $n = 3$, data was presented as the mean ± standard deviation. *$p < 0.05$, **$p < 0.01$, ***$p < 0.001$ *vs* control. PPh3, triphenylphosphine; V-FITC, Annexin V-Fluorescein Isothiocyanate; PI, propidium iodide.

Results

AuPT Time-Dependently Reduces Malignant Phenotype of Human PC3 Cells and Promotes Cell Apoptosis

To explore the effect of AuPT on PCa progression, AuPT concentration was first confirmed. Human PC3 cells were treated with different AuPT concentrations. The results of the cell viability assay showed that the proliferation ability was 50% restrained by 2 μM AuPT, which was considered as the most suitable working concentration (Fig. 1A). After treatment with 2 μM AuPT, the proliferation ability was time-dependently inhibited (Fig. 1B, $p < 0.05$, $p < 0.01$). Next, compared with the control (non-AuPT treatment), the wound healing and relative invasion rate of human PC3 cells decreased after AuPT treatment, which were most prominent 24 h after AuPT intervention (Fig. 1C,D, $p < 0.05$, $p < 0.01$). In addition, the results of flow cytometry show that cell apoptosis significantly increased after treatment with 2 μM AuPT (Fig. 1E, $p < 0.01$). These results indicated that AuPT significantly inhibited the malignant phenotype of human PC3 cells and selectively and time-dependently induced caspase-dependent apoptosis.

Downregulation of Expression of Apoptosis-Related Protein after AuPT Treatment

Because cell apoptosis was affected by AuPT treatment, we further measured the expression levels of apoptosis-related proteins using Western blotting. The results showed that the levels of the proapoptotic proteins Bax ($p < 0.05$, $p < 0.01$, $p < 0.001$) and caspase-3 ($p < 0.01$, $p < 0.001$) in the AuPT-treated group were significantly higher than those in the control group, and the levels were time-dependent. The level of the antiapoptosis protein Bcl-2 ($p < 0.05$, $p < 0.001$) was lower (Fig. 2). AuPT induces caspase-dependent apoptosis in PCa.

Inhibition of UPS Function with AuPT Treatment

AuPT shows an inhibitory effect in some cancers, which is closely related to ubiquitination [23]. We next explored the changes in UPS function in human PC3 cells using Western blotting analysis. Compared with the control group, the levels of UCHL5 ($p < 0.01$) and USP14 ($p < 0.05$, $p < 0.01$) decreased 9, 12, and 24 h after AuPT treatment, whereas the levels of protease substrate p27 ($p < 0.01$) and p53 ($p < 0.001$) were upregulated 6, 9, 12, and 24 h after AuPT treatment. The levels of unfolded protein CHOP ($p < 0.05$, $p < 0.01$) and Bip ($p < 0.05$, $p < 0.01$) were increased 9, 12, and 24 h after AuPT treatment (Fig. 3). These results suggest that AuPT disturbs proteasomal and nonproteasomal functions in PCa cell lines.

Inhibition of NF-κB Pathway with AuPT Treatment

The NF-κB signaling pathway is involved in many complicated physiological processes, including cancer progression, in which ubiquitination and deubiquitination both play critical regulatory roles [24]. p65 is a critical transcription factor in the NF-κB family [25]. We assessed the level of the NF-κB signaling-pathway-related protein, p65, which was compared with that of the control group. The phosphorylation level of p65 gradually and time-dependently decreased, which indicated that the AuPT treatment inhibited the activation of the NF-κB signaling pathway (Fig. 4, $p < 0.05$, $p < 0.01$, $p < 0.001$).

AuPT Inhibits PCa Growth in Vivo

We observed that the malignant phenotype of human PC3 cells was time-dependently inhibited by AuPT treatment *in vitro*. The effect of AuPT on cancer growth was measured by establishing a PCa xenograft nude mouse model. At the end of the treatment period, the tumor tissues were collected and photographed (Fig. 5A). The tumor weight and volume in the high-dose AuPT group were significantly lower than those in the control group (Fig. 5B,C, $p < 0.05$, $p < 0.01$). Furthermore, the results of immunohistochemistry analysis revealed that Ki67 levels were much lower, and the AuPT high-dose treatment was more effective (Fig. 5D).

Deubiquitylating enzymes play key roles in the regulation of cancer progression [26]. UCHL5, an isomer of ubiquitin carboxyl-terminal hydrolase, is important for regulating tumor-related signaling [27]. USP14 participates in the regulation of cancer proliferation and metastasis [28]. Next, we examined UCHL5 and USP14 expressions in AuPT-treated PCa xenograft nude mice. The results of Western blotting analysis revealed that UCHL5 and USP14 levels were lower in the treated mice than those in the control group (Fig. 5E, $p < 0.05$, $p < 0.001$, respectively). These results are consistent with the inhibition of the malignant phenotype of human PC3 cells.

AuPT Downregulates Expressions of UCHL5 and USP14 to Inhibit Malignant Phenotype of PC3 Cell Line

To confirm whether AuPT affects human PC3 cell growth by inhibiting UCHL5 and USP14 expression, an overexpression model was constructed. UCHL5 and USP14 levels were significantly higher in overexpressed PC3 cells than in control cells (Fig. 6A, $p < 0.001$). Carbobenzoxy-valyl-alanyl-aspartyl-[O-methyl] (zVAD), a specific caspase inhibitor, was used to block apoptosis [29]. Cell viability was determined using a CCK-8 assay for the different treatments. We found that the proliferation of human PC3 cells was effectively enhanced by AuPT + zVAD treatment ($p < 0.01$) or by the overexpression of UCHL5 ($p < 0.01$) or USP14 ($p < 0.05$) (Fig. 6B). The migration and invasion abilities of human PC3 cells were significantly re-

Journal of
BIOLOGICAL REGULATORS
and Homeostatic Agents

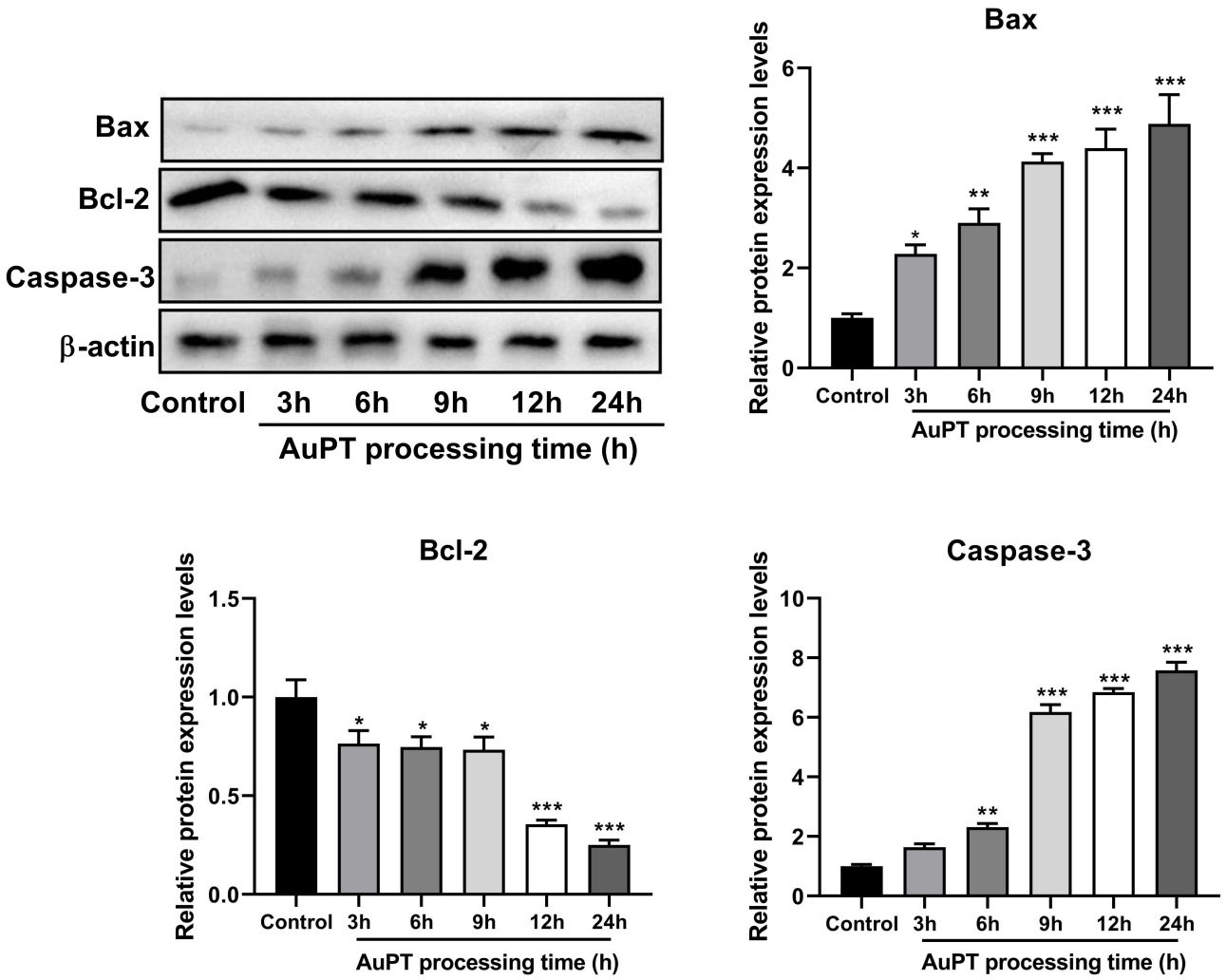

Fig. 2. Downregulation of the expression of apoptosis-related protein under AuPT treatment. Western blotting analyzed protein expression of Bax, Bcl-2 and Caspase-3 at the AuPT processing time in human PC3 cells. $n = 3$, data was presented as the mean ± standard deviation. *$p < 0.05$, **$p < 0.01$, ***$p < 0.001$ *vs* control. Bax, BCL2-associated X; Bcl-2, B-cell lymphoma-2.

stored by cotreatment with AuPT + zVAD ($p < 0.001$) and AuPT + oe-UCHL5 or AuPT + oe-USP14 ($p < 0.01$, $p < 0.001$) (Fig. 6C,D). The rate of apoptosis was significantly lower in the AuPT + zVAD, AuPT + oe-UCHL5, and AuPT + USP14 groups than in the control (Fig. 6E, $p < 0.001$). These results illustrate that AuPT inhibits the expression of UCHL5 and USP14 to attenuate the malignant phenotype of PC3 cells and induces caspase-dependent apoptosis in the PC3 cell line.

AuPT Disturbs UPS Function via Downregulating UCHL5 and USP14 Expression

We found that AuPT downregulated the expressions of DUBs UCHL5 and USP14 both *in vitro* and *in vivo*. Next, we investigated the regulatory role of AuPT on the effects of UCHL5 and USP14 on UPS function. The results showed that the levels of proteasome substrate (p27 and p53) and unfolded proteins (CHOP and Bip) were reversed in the AuPT + zVAD group ($p < 0.001$) and AuPT + oe-UCHL5 or AuPT + USP14 groups compared with those in the control groups ($p < 0.01$, $p < 0.001$) (Fig. 7), demonstrating that AuPT inhibited the expressions of UCHL5 and USP14 and further disturbed the UPS functioning in PC3 cell lines.

AuPT Downregulates NF-κB Pathway by Inhibiting UCHL5 and USP14 Expression

We also found that AuPT downregulated the phosphorylation level of p65. Subsequently, we explored the regulatory role of AuPT in the effects of UCHL5 and USP14 on the NF-κB signaling pathway. The results showed that the phosphorylation level of p65 was reduced with AuPT treatment and was strongly restored with zVAD, oe-UCHL5, or oe-USP14 treatment (Fig. 8, $p < 0.001$). These results indicate that AuPT disturbs UPS functioning to inhibit the activation of the NF-κB pathway.

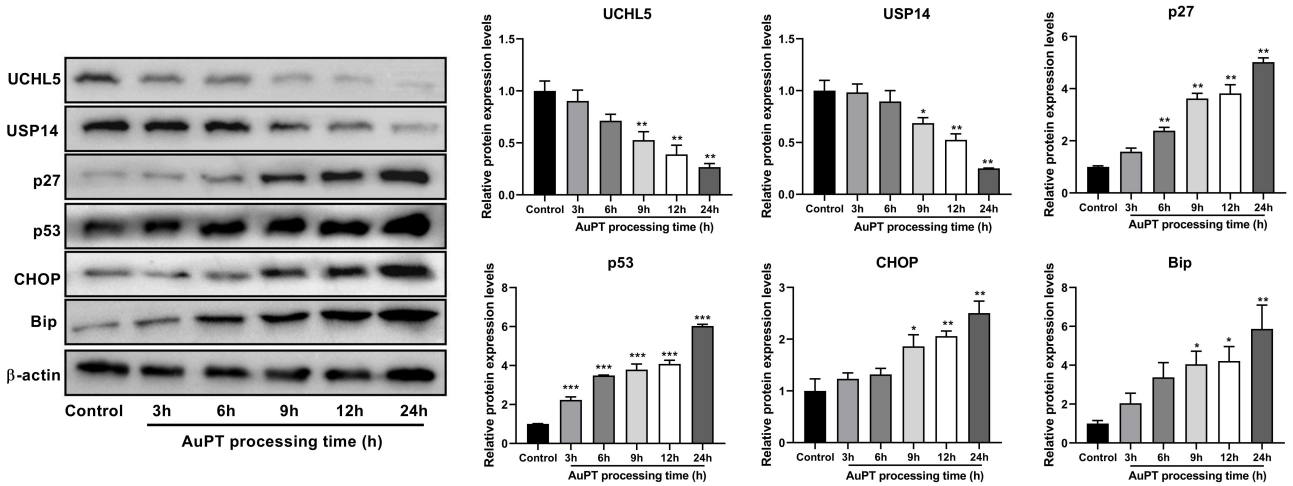

Fig. 3. Inhibition of ubiquitin-proteasome system (UPS) function under AuPT treatment. Western blotting analyzed protein expression levels of deubiquitinated proteins (UCHL5 and USP14), protease substrates (p27 and p53) and unfolded proteins (CHOP and Bip) at the AuPT processing time in human PC3 cells. $n = 3$, data was presented as the mean ± standard deviation. $*p < 0.05$, $**p < 0.01$, $***p < 0.001$ *vs* control. UCHL5, ubiquitin carboxy-terminal hydrolase L5; USP14, ubiquitin-specific protease 14; CHOP, C/EBP-homologous protein; Bip, Heavy-chain binding protein.

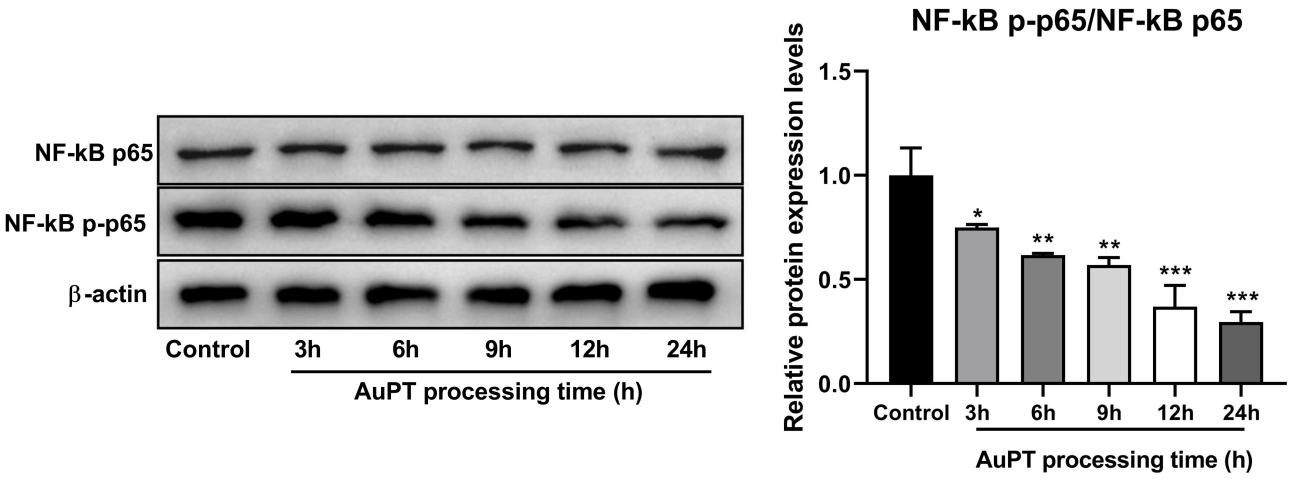

Fig. 4. Inhibition of the nuclear factor-κB (NF-κB) pathway by AuPT. Western blotting analyzed related protein expression of the NF-κB pathway. $n = 3$, data was presented as the mean ± standard deviation. $*p < 0.05$, $**p < 0.01$, $***p < 0.001$ *vs* control.

Discussion

Patients with relapsed or metastatic PCa face considerable medical challenges owing to the emergence of chemotherapy resistance [30]. Thus, anticancer drugs that are safe and highly selective with low cytotoxicity must be studied to prevent the progression of PCa. DUBs play an important role in tumorigenesis, and the inhibition of DUBs is a focus of anticancer medicine research [31]. AuPT was synthesized as an antitumor agent by selectively inhibiting 19S proteasome-associated USP14 and UCHL5 [23]. In this study, we demonstrated that AuPT treatment limits the malignant phenotype of PCa by inducing cell apoptosis and downregulating the NF-κB signaling pathway.

However, reports of DUB inhibitors as effective anticancer agents are rare because of their cytotoxicity, water solubility, and absorbency [32]. EOAI, a specific USP5 inhibitor, can induce lung cancer cell apoptosis, synergistically promote cisplatin chemotherapy, and easily induce resistance [33,34]. 2-N,4-N-dibenzylquinazoline-2,4-diamine (b-AP15), an inhibitor of USP14 or UCH37/UCHL5, induces apoptosis in large B-cell lymphoma cell lines and decreases 5-fluorouracil resistance in colorectal cancer cells; its toxicity is also low [35,36]. Moreover, the highly water-soluble (6 mg/mL) Na-AuPT, a metal-based drug, was synthesized as a proteasome inhibitor that potently inhibited the growth of 11 different types of tumor cells [37]. AuPT induces caspase-

Journal of
BIOLOGICAL REGULATORS
and Homeostatic Agents

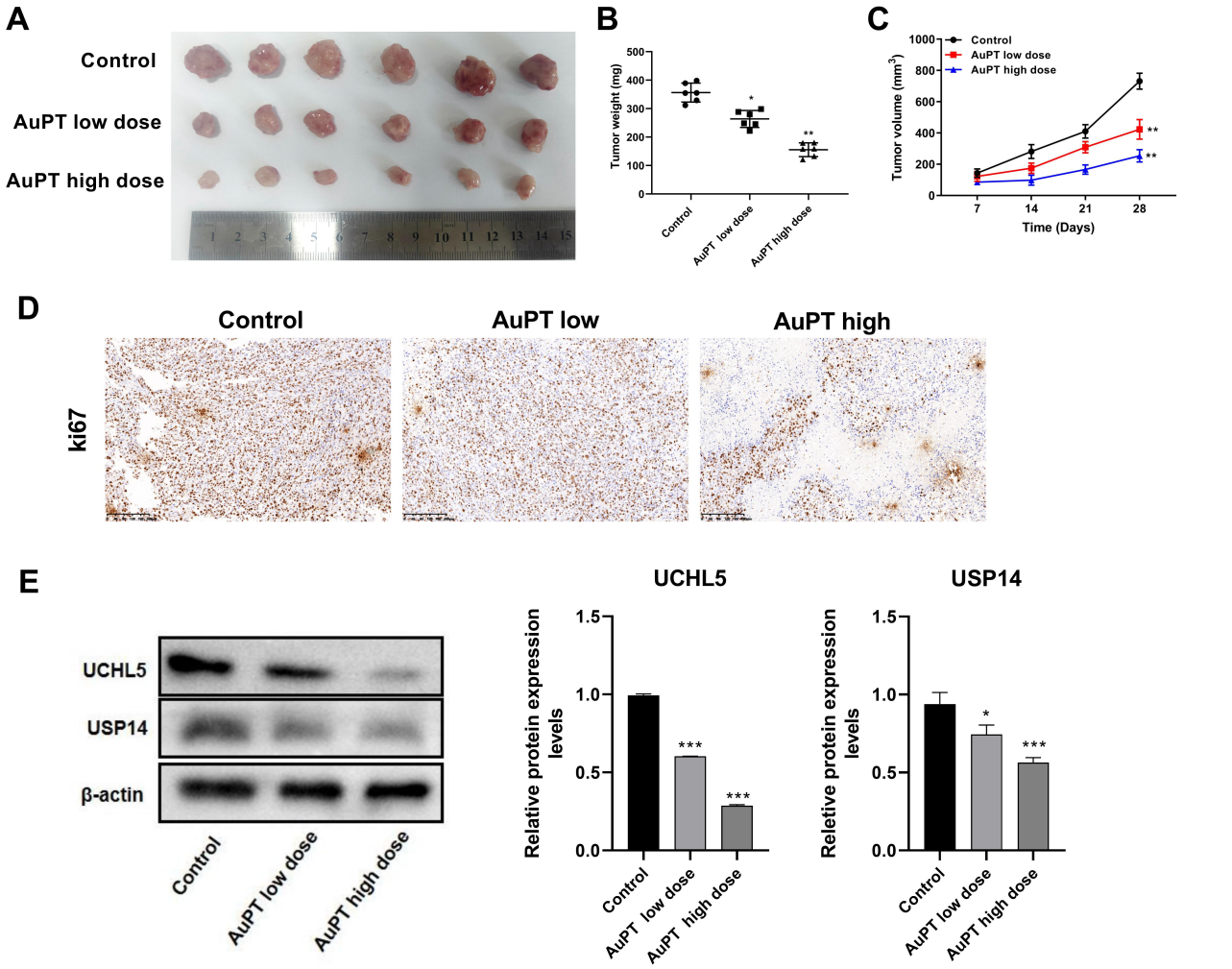

Fig. 5. AuPT inhibits PCa growth in *vivo*. (A) The representative photographs of tumor tissue taken after 4 weeks. (B) Changes in tumor weight were revealed in three groups. (C) Changes in tumor volume were measured once a week. (D) Immunohistochemistry assay examined Ki67 expression in tumor tissue, scale bar (×200): 200 μm. (E) Western blotting analyzed the protein expression level of UCHL5 and USP14. *$p < 0.05$, **$p < 0.01$, ***$p < 0.001$ *vs* control.

dependent apoptosis, showing higher selectivity in inhibiting cancer cell growth than nickel pyrithione or copper pyrithione [23,38,39]. In this study, we found that AuPT strongly inhibited the malignant phenotype of human PC3 cells, promoted apoptotic cell death, and effectively reduced tumor weight and volume in a nude mouse model. These findings indicate that AuPT, as an anticancer drug treatment for PCa, may be more effective and safe, especially given its low cytotoxicity. Further AuPT applications in cancer treatment must be fully tested through clinical trials.

Plasmid transfection was used to verify the roles of USP14 and UCHL5 in PCa progression. The results showed that, in addition to zVAD intervention, the overexpression of USP14 or UCHL5 strongly restored the malignant phenotype of PC3 cells. Targeting USP14 or UCHL5 as an anticancer agent can drive key biological events that inhibit cancer growth. For example, b-AP15 selectively inhibits the activity of UCHL5 to suppress ovarian cancer growth by downregulating transforming growth factor-β/Smad signaling [40]. In addition, UCHL5 knockdown suppressed endometrial cancer growth via the wingless/integrated/β-catenin pathway [41]. Auranofin targets UCHL5 and USP14 to inhibit PCa growth by downregulating AR signaling [42]. These findings provide new insights for the development of specific DUB inhibitors as cancer therapy.

The activation of the NF-κB pathway plays a positive role in tumor metastasis and angiogenesis [37]. Malignant tumors such as PCa usually present with hyperactivation of the NF-κB pathway, which stimulates tumor cell proliferation and invasion [43]. AR signaling is controlled by the NF-κB pathway, which promotes the progression of PCa to castration-resistant PCa [44]. Chelerythrine in-

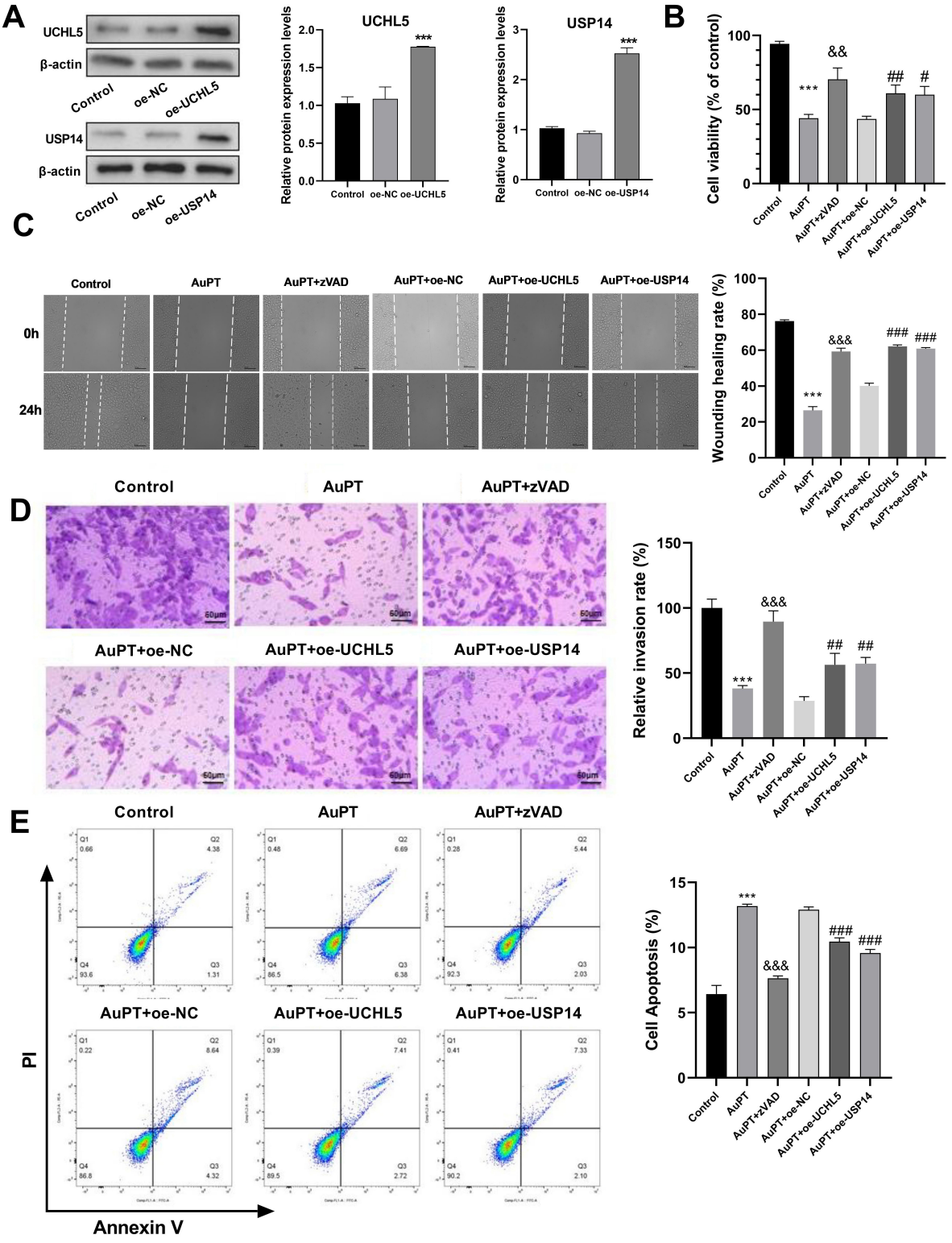

Fig. 6. AuPT downregulates the expression of UCHL5 and USP14 to inhibit malignant phenotype of PC3 cell lines. (A) Western blotting verified protein expression of UCHL5 and USP14 after transfection. Cells were divided into 6 groups under different treatment: the control, AuPT, AuPT + zVAD, AuPT + oe-NC, AuPT + oe-UCHL5 and AuPT + oe-USP14. CCK-8 assay (B), wound healing assay (C) and transwell assay. Scale bar: 50 μm. (D) Examined the viability, migration and invasion ability of PC3 cells under AuPT or zVAD or transfection treatment, respectively. Scale bar: 50 μm. (E) Flow cytometry measured cell apoptosis under different treatment. $^{***}p < 0.001$ *vs* control; $^{\&\&}p < 0.01$, $^{\&\&\&}p < 0.001$ *vs* AuPT; $^{\#}p < 0.05$, $^{\#\#}p < 0.01$, $^{\#\#\#}p < 0.001$ *vs* AuPT + oe-NC; CCK-8, cell counting kit-8; oe-NC, overexpression-Negative Control; zVAD, Carbobenzoxy-valyl-alanyl-aspartyl-[O-methyl].

Journal of
BIOLOGICAL REGULATORS
and Homeostatic Agents

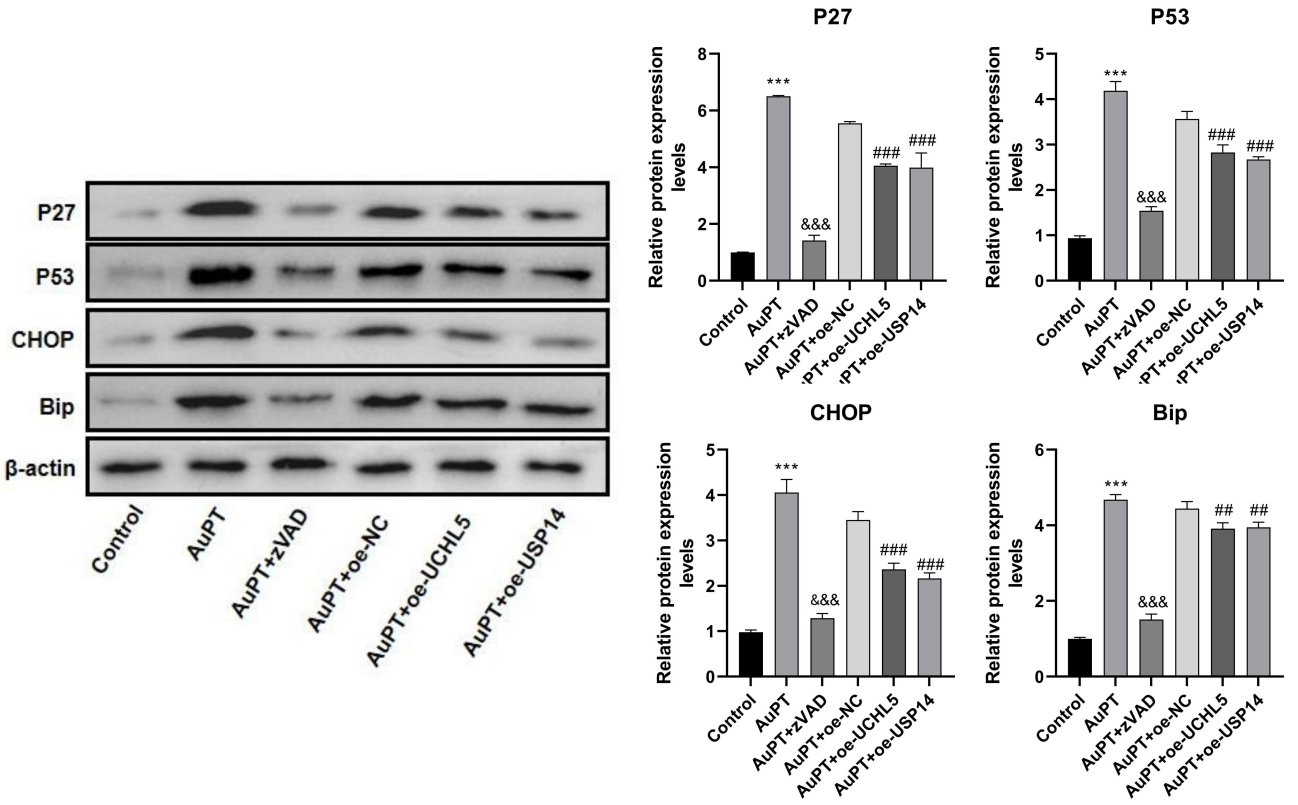

Fig. 7. AuPT disturbs UPS function by downregulating the expression of UCHL5 and USP14. Western blotting assessed protein expression of p27, p53, CHOP and Bip under AuPT or zVAD or transfection treatment. $n = 3$, data was presented as the mean ± standard deviation. $^{***}p < 0.001$ *vs* control; $^{\&\&\&}p < 0.001$ *vs* AuPT; $^{\#\#}p < 0.01$, $^{\#\#\#}p < 0.001$ *vs* AuPT + oe-NC.

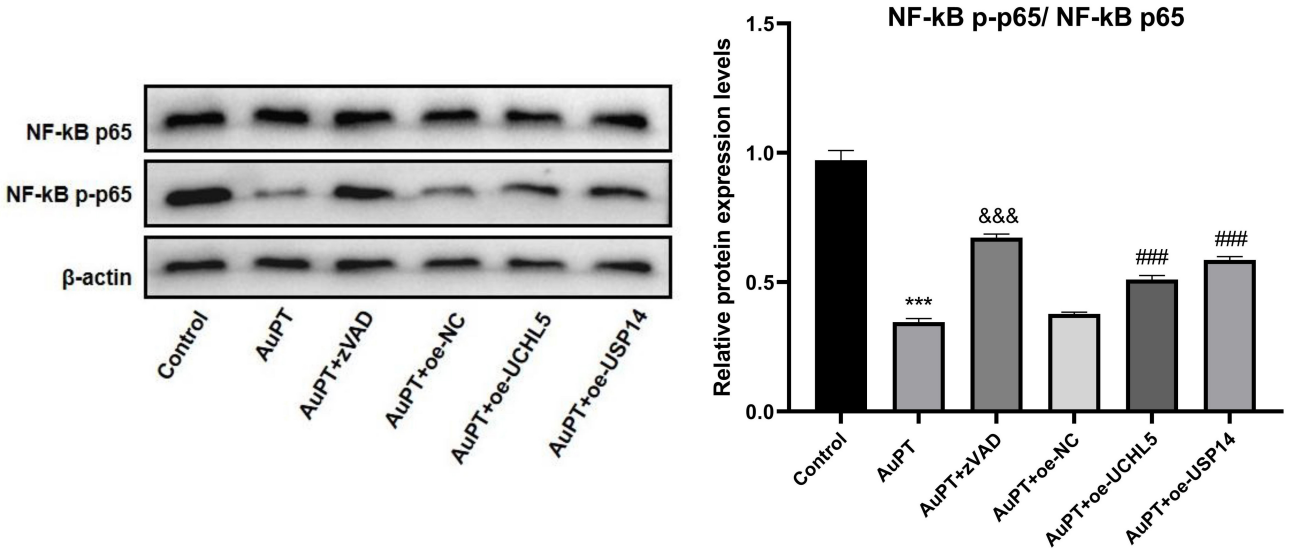

Fig. 8. AuPT downregulates the NF-κB pathway by inhibiting UCHL5 and USP14. Western blotting assessed the related protein expression of the NF-κB pathway under AuPT or transfection. $n = 3$, data was presented as the mean ± standard deviation. $^{***}p < 0.001$ *vs* control; $^{\&\&\&}p < 0.001$ *vs* AuPT; $^{\#\#\#}p < 0.001$ *vs* AuPT + oe-NC.

hibited PC3 cell migration and invasion by decreasing the levels of p65 [45]. Imipramine has a similar effect on the serine/threonine protein kinase-NF-κB signaling pathway [46]. NF-κB p65 is degraded via ubiquitination to suppress breast cancer growth, which demonstrates that UPS can regulate the activity of the NF-κB signaling pathway [16]. In this study, we found that AuPT treatment inhibited the phosphorylation of p65, which was strongly rescued af-

ter zVAD intervention or by the overexpression of UCHL5 or USP14. These findings suggest that the inhibition of the NF-κB signaling pathway can attenuate cancer progression. Taken together, AuPT exerts antitumor effects in PCa and could be a drug for PCa treatment. Additionally, our study provides new insights into the mechanisms of AuPT, and the information obtained will be helpful in expanding the clinical applications of AuPT.

Conclusions

We demonstrated that AuPT significantly inhibited on PC3 cell growth and PCa xenografts in nude mice. The results of further exploration of the mechanisms of this effect showed that AuPT downregulates NF-κB signaling and enhances apoptosis via inhibiting the expression of UCHL5 and USP14 in PCa.

Availability of Data and Materials

All experimental data included in this study can be obtained by contacting the corresponding author if needed.

Author Contributions

HWZ and PZ designed the research study. XHF and DDC performed the research. HWZ and PT provided help and advice on the design experiments. XHF and DDC analyzed the data. All authors contributed to editorial changes in the manuscript. All authors read and approved the final manuscript. All authors have participated sufficiently in the work and agreed to be accountable for all aspects of the work.

Ethics Approval and Consent to Participate

All animal experiments were approved by the Institutional Animal Care and Use Committee of the Guangzhou Medical University (approval number: GY2018-043).

Acknowledgment

Not applicable.

Funding

This research was funded by Guangzhou Municipal Science and Technology Program (No. 201804010453).

Conflict of Interest

The authors declare no conflict of interest.

Supplementary material

Supplementary material associated with this article can be found, in the online version, at https://doi.org/10.23812/j.biol.regul.homeost.agents.20243805.327.

References

[1] Siegel RL, Miller KD, Fuchs HE, Jemal A. Cancer Statistics, 2021. CA: a Cancer Journal for Clinicians. 2021; 71: 7–33.
[2] Sung H, Ferlay J, Siegel RL, Laversanne M, Soerjomataram I, Jemal A, *et al*. Global Cancer Statistics 2020: GLOBOCAN Estimates of Incidence and Mortality Worldwide for 36 Cancers in 185 Countries. CA: a Cancer Journal for Clinicians. 2021; 71: 209–249.
[3] Bergengren O, Pekala KR, Matsoukas K, Fainberg J, Mungovan SF, Bratt O, *et al*. 2022 Update on Prostate Cancer Epidemiology and Risk Factors-A Systematic Review. European Urology. 2023; 84: 191–206.
[4] Catalona WJ. Prostate Cancer Screening. The Medical Clinics of North America. 2018; 102: 199–214.
[5] Beer TM, Armstrong AJ, Rathkopf DE, Loriot Y, Sternberg CN, Higano CS, *et al*. Enzalutamide in metastatic prostate cancer before chemotherapy. The New England Journal of Medicine. 2014; 371: 424–433.
[6] de Bono JS, Logothetis CJ, Molina A, Fizazi K, North S, Chu L, *et al*. Abiraterone and increased survival in metastatic prostate cancer. The New England Journal of Medicine. 2011; 364: 1995–2005.
[7] Antonarakis ES, Lu C, Wang H, Luber B, Nakazawa M, Roeser JC, *et al*. AR-V7 and resistance to enzalutamide and abiraterone in prostate cancer. The New England Journal of Medicine. 2014; 371: 1028–1038.
[8] Komander D, Clague MJ, Urbé S. Breaking the chains: structure and function of the deubiquitinases. Nature Reviews. Molecular Cell Biology. 2009; 10: 550–563.
[9] Clague MJ, Urbé S, Komander D. Breaking the chains: deubiquitylating enzyme specificity begets function. Nature Reviews. Molecular Cell Biology. 2019; 20: 338–352.
[10] Lee MJ, Lee BH, Hanna J, King RW, Finley D. Trimming of ubiquitin chains by proteasome-associated deubiquitinating enzymes. Molecular & Cellular Proteomics: MCP. 2011; 10: R110.003871.
[11] Yang Y, Cao L, Guo Z, Gu H, Zhang K, Qiu Z. Deubiquitinase UCHL5 stabilizes ELK3 to potentiate cancer stemness and tumor progression in pancreatic adenocarcinoma (PAAD). Experimental Cell Research. 2022; 421: 113402.
[12] Lv C, Wang S, Lin L, Wang C, Zeng K, Meng Y, *et al*. USP14 maintains HIF1-α stabilization via its deubiquitination activity in hepatocellular carcinoma. Cell Death & Disease. 2021; 12: 803.
[13] Du XH, Ke SB, Liang XY, Gao J, Xie XX, Qi LZ, *et al*. USP14 promotes colorectal cancer progression by targeting JNK for stabilization. Cell Death & Disease. 2023; 14: 56.
[14] Aggarwal BB, Sung B. NF-κB in cancer: a matter of life and death. Cancer Discovery. 2011; 1: 469–471.
[15] Yu H, Lin L, Zhang Z, Zhang H, Hu H. Targeting NF-κB pathway for the therapy of diseases: mechanism and clinical study. Signal Transduction and Targeted Therapy. 2020; 5: 209.
[16] Ren C, Han X, Lu C, Yang T, Qiao P, Sun Y, *et al*. Ubiquitination of NF-κB p65 by FBXW2 suppresses breast cancer stemness, tumorigenesis, and paclitaxel resistance. Cell Death and Differentiation. 2022; 29: 381–392.
[17] Xiong W, Gao X, Zhang T, Jiang B, Hu MM, Bu X, *et al*. USP8 inhibition reshapes an inflamed tumor microenvironment that potentiates the immunotherapy. Nature Communications. 2022; 13: 1700.
[18] Man X, Piao C, Lin X, Kong C, Cui X, Jiang Y. USP13 functions as a tumor suppressor by blocking the NF-kB-mediated PTEN downregulation in human bladder cancer. Journal of Experimental & Clinical Cancer Research: CR. 2019; 38: 259.
[19] Li B, Qi ZP, He DL, Chen ZH, Liu JY, Wong MW, *et al*.

Journal of
BIOLOGICAL REGULATORS
and Homeostatic Agents

NLRP7 deubiquitination by USP10 promotes tumor progression and tumor-associated macrophage polarization in colorectal cancer. Journal of Experimental & Clinical Cancer Research: CR. 2021; 40: 126.

[20] Chen D, Milacic V, Frezza M, Dou QP. Metal complexes, their cellular targets and potential for cancer therapy. Current Pharmaceutical Design. 2009; 15: 777–791.

[21] Chen X, Yang Q, Xiao L, Tang D, Dou QP, Liu J. Metal-based proteasomal deubiquitinase inhibitors as potential anticancer agents. Cancer Metastasis Reviews. 2017; 36: 655–668.

[22] Galluzzi L, Senovilla L, Vitale I, Michels J, Martins I, Kepp O, *et al*. Molecular mechanisms of cisplatin resistance. Oncogene. 2012; 31: 1869–1883.

[23] Li X, Huang Q, Long H, Zhang P, Su H, Liu J. A new gold(I) complex-Au(PPh_3)PT is a deubiquitinase inhibitor and inhibits tumor growth. EBioMedicine. 2019; 39: 159–172.

[24] Al-Rashidi RR, Noraldeen SAM, Kareem AK, Mahmoud AK, Kadhum WR, Ramírez-Coronel AA, *et al*. Malignant function of nuclear factor-kappaB axis in prostate cancer: Molecular interactions and regulation by non-coding RNAs. Pharmacological Research. 2023; 194: 106775.

[25] Hayden MS, Ghosh S. Shared principles in NF-kappaB signaling. Cell. 2008; 132: 344–362.

[26] D'Arcy P, Brnjic S, Olofsson MH, Fryknäs M, Lindsten K, De Cesare M, *et al*. Inhibition of proteasome deubiquitinating activity as a new cancer therapy. Nature Medicine. 2011; 17: 1636–1640.

[27] Wang S, Wang T, Yang Q, Cheng S, Liu F, Yang G, *et al*. Proteasomal deubiquitylase activity enhances cell surface recycling of the epidermal growth factor receptor in non-small cell lung cancer. Cellular Oncology (Dordrecht). 2022; 45: 951–965.

[28] Wang F, Ning S, Yu B, Wang Y. USP14: Structure, Function, and Target Inhibition. Frontiers in Pharmacology. 2022; 12: 801328.

[29] Slee EA, Zhu H, Chow SC, MacFarlane M, Nicholson DW, Cohen GM. Benzyloxycarbonyl-Val-Ala-Asp (OMe) fluoromethylketone (Z-VAD.FMK) inhibits apoptosis by blocking the processing of CPP32. The Biochemical Journal. 1996; 315: 21–24.

[30] Seruga B, Ocana A, Tannock IF. Drug resistance in metastatic castration-resistant prostate cancer. Nature Reviews. Clinical Oncology. 2011; 8: 12–23.

[31] Manasanch EE, Orlowski RZ. Proteasome inhibitors in cancer therapy. Nature Reviews. Clinical Oncology. 2017; 14: 417–433.

[32] Love KR, Catic A, Schlieker C, Ploegh HL. Mechanisms, biology and inhibitors of deubiquitinating enzymes. Nature Chemical Biology. 2007; 3: 697–705.

[33] Zheng Y, Wang L, Niu X, Guo Y, Zhao J, Li L, *et al*. EOAI, a ubiquitin-specific peptidase 5 inhibitor, prevents non-small cell lung cancer progression by inducing DNA damage. BMC Cancer. 2023; 23: 28.

[34] Takahara PM, Rosenzweig AC, Frederick CA, Lippard SJ. Crystal structure of double-stranded DNA containing the major adduct of the anticancer drug cisplatin. Nature. 1995; 377: 649–652.

[35] Jiang L, Sun Y, Wang J, He Q, Chen X, Lan X, *et al*. Proteasomal cysteine deubiquitinase inhibitor b-AP15 suppresses migration and induces apoptosis in diffuse large B cell lymphoma. Journal of Experimental & Clinical Cancer Research: CR. 2019; 38: 453.

[36] Ding W, Wang JX, Wu JZ, Liu AC, Jiang LL, Zhang HC, *et al*. Targeting proteasomal deubiquitinases USP14 and UCHL5 with b-AP15 reduces 5-fluorouracil resistance in colorectal cancer cells. Acta Pharmacologica Sinica. 2023; 44: 2537–2548.

[37] Xu DC, Yang L, Zhang PQ, Yan D, Xue Q, Huang QT, *et al*. Pharmacological characterization of a novel metal-based proteasome inhibitor Na-AuPT for cancer treatment. Acta Pharmacologica Sinica. 2022; 43: 2128–2138.

[38] Liu N, Liu C, Li X, Liao S, Song W, Yang C, *et al*. A novel proteasome inhibitor suppresses tumor growth via targeting both 19S proteasome deubiquitinases and 20S proteolytic peptidases. Scientific Reports. 2014; 4: 5240.

[39] Lan X, Zhao C, Chen X, Zhang P, Zang D, Wu J, *et al*. Nickel pyrithione induces apoptosis in chronic myeloid leukemia cells resistant to imatinib via both Bcr/Abl-dependent and Bcr/Abl-independent mechanisms. Journal of Hematology & Oncology. 2016; 9: 129.

[40] Fukui S, Nagasaka K, Miyagawa Y, Kikuchi-Koike R, Kawata Y, Kanda R, *et al*. The proteasome deubiquitinase inhibitor bAP15 downregulates TGF-β/Smad signaling and induces apoptosis *via* UCHL5 inhibition in ovarian cancer. Oncotarget. 2019; 10: 5932–5948.

[41] Liu D, Song Z, Wang X, Ouyang L. Ubiquitin C-Terminal Hydrolase L5 (UCHL5) Accelerates the Growth of Endometrial Cancer via Activating the Wnt/β-Catenin Signaling Pathway. Frontiers in Oncology. 2020; 10: 865.

[42] Liu N, Guo Z, Xia X, Liao Y, Zhang F, Huang C, *et al*. Auranofin lethality to prostate cancer includes inhibition of proteasomal deubiquitinases and disrupted androgen receptor signaling. European Journal of Pharmacology. 2019; 846: 1–11.

[43] Taniguchi K, Karin M. NF-κB, inflammation, immunity and cancer: coming of age. Nature Reviews. Immunology. 2018; 18: 309–324.

[44] Thomas-Jardin SE, Dahl H, Nawas AF, Bautista M, Delk NA. NF-κB signaling promotes castration-resistant prostate cancer initiation and progression. Pharmacology & Therapeutics. 2020; 211: 107538.

[45] Yang B, Zhang D, Qian J, Cheng Y. Chelerythrine suppresses proliferation and metastasis of human prostate cancer cells via modulating MMP/TIMP/NF-κB system. Molecular and Cellular Biochemistry. 2020; 474: 199–208.

[46] Lim EY, Park J, Kim YT, Kim MJ. Imipramine Inhibits Migration and Invasion in Metastatic Castration-Resistant Prostate Cancer PC-3 Cells via AKT-Mediated NF-κB Signaling Pathway. Molecules (Basel, Switzerland). 2020; 25: 4619.